EasyChair Preprint

№ 13989

Research on Train Track Vibration Localization Method Based on Weak Light Grating Array Sensing

Liang Xin, Xiaojun Tang, Lixia Liu, Tianli Hui, Tigang Ning and Bingbing Zhang

July 16, 2024

Research on Train Track Vibration Localization Method Based on Weak Light Grating Array Sensing

1st Liang Xin*

Beijing Satellite Manufacturing Co. , Ltd.

Beijing jiaotong university

Beijing, China

23111040@bjtu.edu.cn

2nd Xiaojun Tang

Beijing Satellite Manufacturing Co. , Ltd.

Beijing jiaotong university

Beijing, China

1248198969@qq.com

3rd Lixia Liu

Beijing Satellite Manufacturing Co. , Ltd.

Beijing jiaotong university

Beijing, China

Zhangbb_cidp@163.com

4th Tianli Hui

Beijing Satellite Manufacturing Co. , Ltd.

Beijing jiaotong university

Beijing, China

zhangbbcidp@163.com

5th Tigang Ning

Beijing jiaotong university

Beijing Satellite Manufacturing Co. , Ltd.

Beijing, China

tgning@bjtu.edu.cn

6th Bingbing Zhang

Beijing jiaotong university

Beijing Satellite Manufacturing Co. , Ltd.

Beijing, China

15731338004@163.com

***Abstract*—To address these issues, this paper combines the characteristics of fiber Bragg gratings such as insulation, strong anti-interference capability, and corrosion resistance, and employs weak grating array technology to construct a piezoelectric ceramic testing system. The frequency response and phase amplitude of this system are verified. By setting up a field test environment, the localization effect of the weak grating array is validated. The test results indicate that the weak grating array encapsulated in the track can clearly perceive track vibrations and achieve vibration localization. In future research, this technology is expected to achieve functions such as train speed measurement, localization, foreign object intrusion detection, and track defect detection.**

Keywords—Railway Transportation; Localization; Weak Grating; Vibration

I. INTRODUCTION

Currently, traditional wheel-rail trains primarily use photoelectric encoders or speed measuring motors installed at the axle ends to convert the rotation of train wheels into speed data. This data is then read and combined with methods like track circuits, balises, or wireless communication to determine the train's position [1]. In contrast, maglev trains, which utilize electromagnetic forces for levitation, guidance, and propulsion, do not have contact between the train body and the track. As a result, the speed and positioning methods based on wheel-rail contact used for traditional trains are not applicable to maglev trains [2]. Existing maglev train speed measurement and positioning technologies, such as those based on counting sleepers for speed measurement and using long stator slot detection for relative positioning, face significant challenges. Over long distances, these methods accumulate errors that severely impact the results and are easily influenced by external factors [3-5]. Other approaches, like using the Global Navigation Satellite System (GNSS) for speed measurement and localization, or absolute positioning technologies based on query-response systems and pulse width coding, provide high accuracy but come with high equipment and maintenance costs [6-7].

Fiber Bragg grating (FBG) sensors possess inherent insulation properties, making them superior to other electrical systems due to their strong anti-interference capability, low cost, corrosion resistance, and fast response time [8-9]. These characteristics make FBG sensors particularly suitable for complex environments and long-distance monitoring applications. Phase-sensitive optical time-domain reflectometry (φ-OTDR) is a commonly used technology in distributed FBG sensing, offering high sensitivity and a broad monitoring range [10]. However, this system demodulates changes in the backscattered Rayleigh signals within the

sensing fiber. Due to the low Rayleigh scattering coefficient in the fiber, it is highly susceptible to external interference, leading to false alarms [11-12]. Compared to distributed fiber sensing methods based on backscattering, quasi-distributed fiber sensing technology using FBGs provides a higher signal-to-noise ratio and physical localization characteristics [13-14]. When combined with various multiplexing techniques, it can support the construction of large-scale sensing networks [15-16]. FBG sensors achieve absolute localization requirements for grating points through dense multiplexing. The spacing between different gratings determines the positioning accuracy, and a low reflectivity FBG array can enable thousands of weak gratings to sense simultaneously on a single fiber [17-18], offering a viable solution for train positioning and speed measurement.

In this paper, we combine the concept of Distributed Acoustic Sensing (DAS) with weak gratings as reflective interference sources (uwDAS) and the characteristics of fiber Bragg gratings, such as insulation, strong anti-interference capability, and corrosion resistance. Using weak grating array technology, we constructed a piezoelectric ceramic testing system and validated its frequency response and phase amplitude. By setting up a field test environment, we verified the localization effectiveness of the weak grating array. The test results indicate that the weak grating array encapsulated in the track can clearly sense track vibrations and achieve vibration localization.

II. Theoretical Analysis of Weak Fiber Grating Array Sensing Principle

A. Multiple Reflection Interference

In a single optical fiber, light undergoes multiple reflections between various fiber Bragg gratings (FBGs). This results in light that has undergone multiple reflections interfering with light that has only reflected once, both returning to the photodetector and creating noise that interferes with the measurement signal. Fig. 1 illustrates four reflection paths. Compared to the reflection path of FBG4, the other three paths include one additional round-trip reflection, referred to as first-order reflections. Reflections involving more than one additional round-trip process are called higher-order reflections. In an FBG array, second-order and higher-order reflections are very weak, so typically only the effects of first-order reflections are considered.

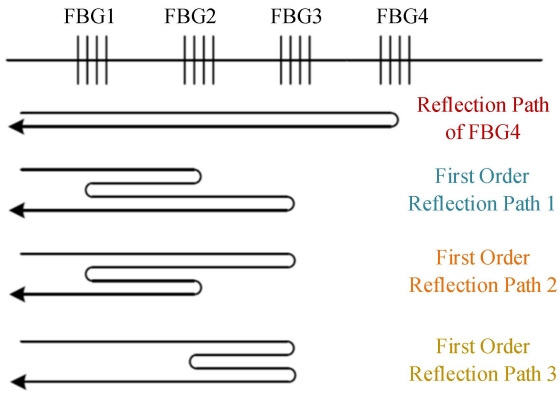

Fig. 1. Four Reflection Paths

Identify applicable funding agency here. If none, delete this text box.

When the reflectivity of each fiber Bragg grating (FBG) in the grating array is the same, the first-order reflection signal of the *i*-th grating is given by:

$$G_i(\lambda) = \frac{(i-1)(i-2)}{2} R^3(\lambda)\ I_0(\lambda)[1-R^3(\lambda)]^{2(i-2)} \quad (1)$$

Exactly. Lower reflectivity of the fiber Bragg gratings (FBGs) results in less influence from multiple reflections on the measurement signal. Therefore, to minimize cross-talk from multiple reflections, it is advisable to reduce the reflectivity of the FBGs appropriately, utilizing weakly reflecting fiber Bragg gratings.

B. Weak Fiber Grating Array

The full name of weak fiber Bragg gratings (FBGs) is weakly reflecting fiber Bragg gratings, with a reflectivity as low as 0.1%. This ensures that light passing through the previous weakly reflecting FBG still maintains sufficient intensity to propagate backward. Simultaneously, it effectively suppresses shadow effects and cross-talk from higher-order reflections. The low reflectivity of weakly reflecting FBGs facilitates large-scale multiplexing of FBGs, significantly reducing the requirements for light source bandwidth and power. This condition enhances the potential for increasing the number of FBG multiplexing, facilitating long-distance and wide-range sensing applications.

The structure of the weak grating array fiber sensing system is illustrated in Fig. 2. A continuous light with a continuously changing wavelength is output from the laser source. It undergoes pulse modulation to become pulsed light, which is then amplified and introduced into the weak grating array. A photodetector collects the reflected light signals from the weak grating array at high frequencies. When the temperature or strain of the FBGs changes, the center wavelength of the reflected light also changes. Therefore, by detecting the wavelength of the reflected light, corresponding strain or temperature information can be obtained.

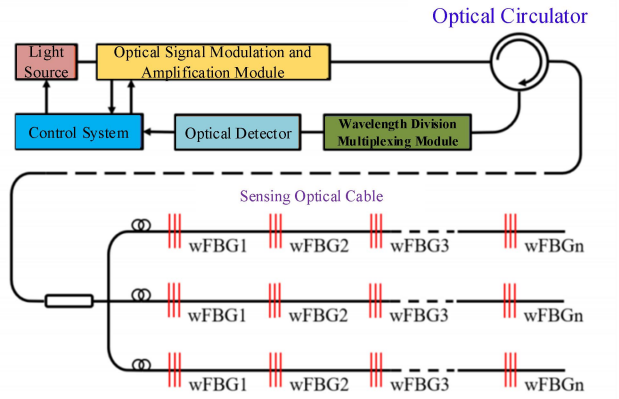

Fig. 2. Structure of the Weak Fiber Grating Array Sensing System

During this process, the weak grating array fiber sensing system utilizes a hybrid multiplexing technique involving wavelength division multiplexing (WDM), time division multiplexing (TDM), and spatial division multiplexing (SDM) for signal detection. According to the principle of SDM, different channels of fiber Bragg gratings (FBGs) alternate

operation under the adjustment of optical switches. Based on the principle of TDM, the light signals reflected by weak FBGs at certain intervals return in a specific time sequence. Following the principle of WDM, multiple weak FBGs with different wavelengths are set up. The WDM module distinguishes the reflected light signals of different wavelengths and directs them to the photodetector, converting them into electrical signals. Consequently, strain or temperature information from the weak FBGs, along with their corresponding positional data, can be obtained.

C. Distributed Vibration Sensing

Phase-sensitive optical time-domain reflectometry (Φ-OTDR) primarily utilizes the backscattered Rayleigh scattering light generated within the optical fiber. When light propagates through the fiber, it experiences an approximate loss of 0.2 dB/km, mainly due to scattering phenomena occurring within the fiber. Rayleigh scattering accounts for about 85% of this loss, with the remaining 15% attributed to Raman scattering and Brillouin scattering. Rayleigh scattering occurs in all directions, and the Rayleigh scattering propagating backward returns along the fiber in the opposite direction, forming the backscattered Rayleigh scattering light.

When external disturbances affect the optical fiber, it undergoes deformation, causing a change in the fiber's effective refractive index. This, in turn, leads to a variation in the phase of the backscattered Rayleigh scattering light. Upon demodulation, the phase change of the backscattered Rayleigh scattering light within the optical fiber can be translated into information regarding the external disturbances.

The phase change can be expressed as:

$$\Delta\varphi = \beta \cdot \Delta L + L \cdot \Delta L = \beta L \cdot \frac{\Delta L}{L} + L \cdot (\frac{\partial \beta}{\partial n})\Delta n + L \cdot (\frac{\partial \beta}{\partial \alpha})\Delta\alpha \quad (2)$$

In the equation, $\Delta\varphi$ represents the phase difference between the Rayleigh scattering light in a certain section of the optical fiber after disturbance and the phase before disturbance. β is a transmission constant, L is the length of the specific section of the optical fiber, n is the refractive index of the fiber, and α is the diameter of the fiber core.

Equation (2) expresses the relationship between the phase change of the Rayleigh scattering light before and after disturbance and the changes in the length, refractive index, and core diameter of the optical fiber. In this equation, the terms corresponding to the refractive index of the fiber and the core diameter are significantly smaller than the term corresponding to the length of the optical fiber. Therefore:

$$\Delta\varphi \approx \beta L \cdot \frac{\Delta L}{L} \quad (3)$$

Equation (3) indicates that within a segment of optical fiber, when light of a certain wavelength undergoes Rayleigh scattering, the phase change of the Rayleigh scattering light before and after disturbance is proportional to the strain in the optical fiber. A common type of phase-demodulation Φ-OTDR system sensing process is illustrated in Fig. 3. Laser light emitted from the laser undergoes modulation to form coherent pulse light. This light is injected into the fiber through the circulator. After external disturbance, the backscattered Rayleigh scattering light interferes with the undisturbed backscattered Rayleigh scattering light and returns to the circulator. It then passes through the circulator and the photodetection module before entering the demodulation module, where external disturbance information is restored.

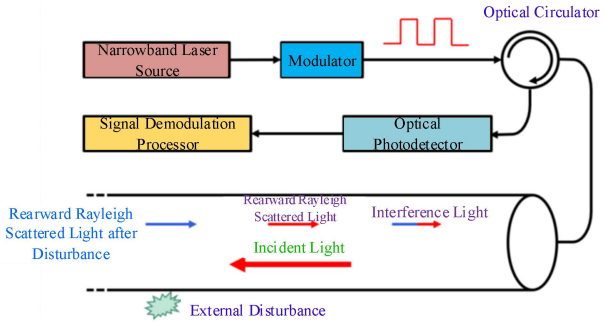

Fig. 3. Structure of the Φ-OTDR Sensing System

In recent years, Distributed Acoustic Sensing (DAS) technology, developed based on Φ-OTDR, has experienced rapid growth in applications. However, Φ-OTDR relies on interference of light to collect vibration information through receiving backscattered Rayleigh scattering signals. The Rayleigh scattering signals are abundant but weak. Extracting the required vibration signals from these signals demands high requirements for both demodulation hardware and software algorithms.

D. Weak Fiber Grating Distributed Vibration Sensing

To overcome the aforementioned challenges, periodic ultra-low reflectivity gratings are inscribed on the sensing fiber. These gratings serve as reflective interference sources, and the signals from adjacent grating points are utilized for interference. With specialized demodulation instruments, the complex Rayleigh scattering signals are replaced by reflective signals. Vibration signals are then extracted, significantly enhancing the dynamic range, monitoring spatial resolution, and signal-to-noise ratio. Compared to traditional DAS, the signal-to-noise ratio of this approach is improved by 20 dB to 30 dB. This technology, which utilizes weak gratings as reflective interference sources in Distributed Acoustic Sensing (DAS), is termed Ultra Weak FBG Distributed Acoustic Sensing (uwDAS).

The uwDAS measurement system, as depicted in Fig. 4, involves a narrowband laser source emitting laser light. This light is modulated to form optical pulses and is then amplified by an erbium-doped fiber amplifier before entering the circulator. The light reflected from the grating positions is interfered with after optical compensation. The interference, carrying vibration signals along the fiber, enters the signal processing unit. By analyzing the phase change of the interference light, a data matrix is formed, allowing for the extraction of acoustic vibration frequency, phase, and amplitude information.

Identify applicable funding agency here. If none, delete this text box.

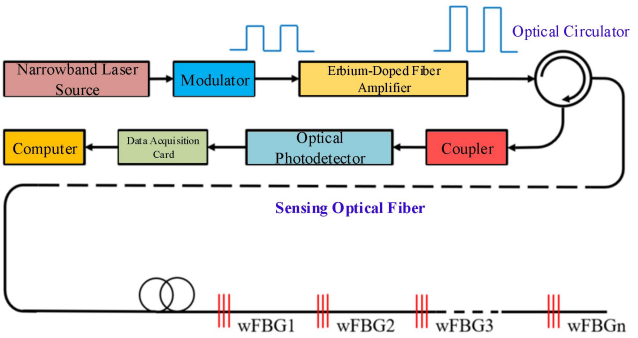

Fig. 4. Structure of the Weak Fiber Grating Distributed Vibration Sensing System

III. Verification of Weak Fiber Grating Characteristics and Vibration Testing

A. Frequency Response Verification

Piezoelectric ceramics undergo slight deformation when subjected to a certain voltage, which is proportional to the external electric field. A piezoelectric ceramic phase modulator, acting on the optical fiber, causes deformation in the fiber corresponding to the deformation in the piezoelectric ceramic, thereby altering the phase of the interference light. Let's consider a piezoelectric ceramic phase modulator with an inner diameter of 80 mm and a radial coefficient of 0.125 um/V.

For the piezoelectric ceramic phase modulator, the signal generator sends fixed voltages of 5 V at frequencies of 5 Hz, 100 Hz, and 1000 Hz. As the frequency increases, the pulse period needs to be reduced to increase the sampling rate and avoid signal distortion. For a pulse frequency of 5 Hz and 100 Hz, a pulse period of 100 microseconds is selected. For a frequency of 1000 Hz, a pulse period of 30 microseconds is used. The frequency domain plots obtained from the demodulation of the uwDAS system are depicted in Fig. 5, it can be observed that the uwDAS system accurately demodulates the external vibration frequencies at 5 Hz, 100 Hz, and 1000 Hz.

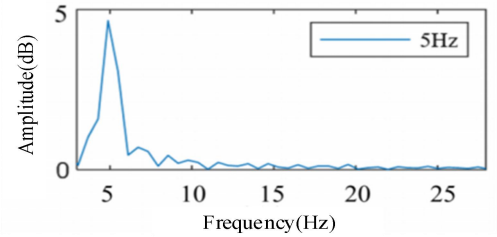

a) Frequency domain plot of demodulated signals at 5 Hz

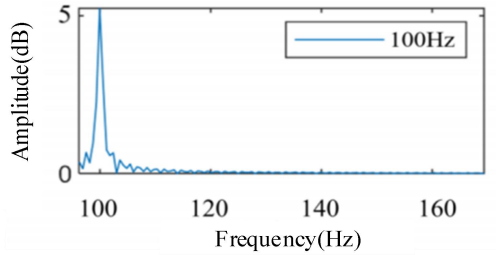

b) Frequency domain plot of demodulated signals at 100 Hz

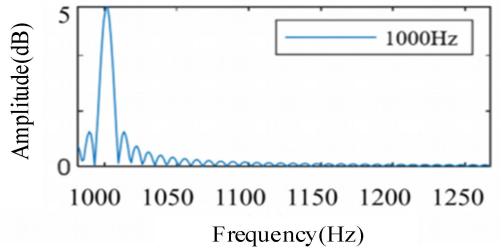

c) Frequency domain plot of demodulated signals at 1000 Hz

Fig. 5. Frequency Domain Plot of Demodulated Signals at Different Frequencies

B. Phase Amplitude Response Verification

The piezoelectric ceramic phase modulator signal generator sends a fixed-frequency sine wave signal at 200 Hz. The voltage is gradually increased from 1 V to 10 V in steps of 1 V. The voltage of the signal generator and the phase of the demodulated signal from the uwDAS system are recorded, as shown by the data points in Fig. 6. The phase amplitude of the demodulated signal shows a linear relationship with the voltage of the signal generator. A linear fit is applied to the data points, as shown by the fitted line in Fig. 6, with an R-squared value of 0.999, indicating a high degree of linearity.

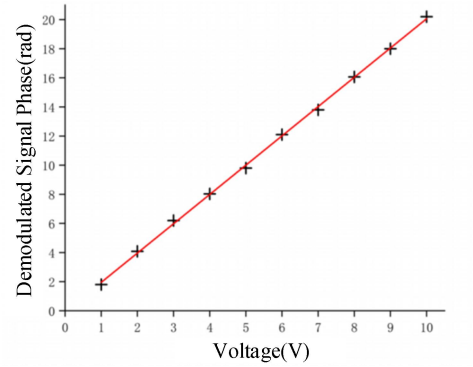

Fig. 6. Phase Amplitude Variation with Voltage

C. Location Test

The weak fiber grating array is embedded in a cement pit beside the track, with the pit measuring 20 meters in length. Four specific grating points are designated as ONML, while the remaining grating measurement points are freely placed on the track. The tail end of the weak fiber grating array is located 200 meters from the starting point, as illustrated in Fig. 7. During the experiment, a rubber mallet is used to strike different positions along the track to observe the vibration response of the weak fiber grating array.

Fig. 7. Deployment of Fiber Grating Array and Field Testing

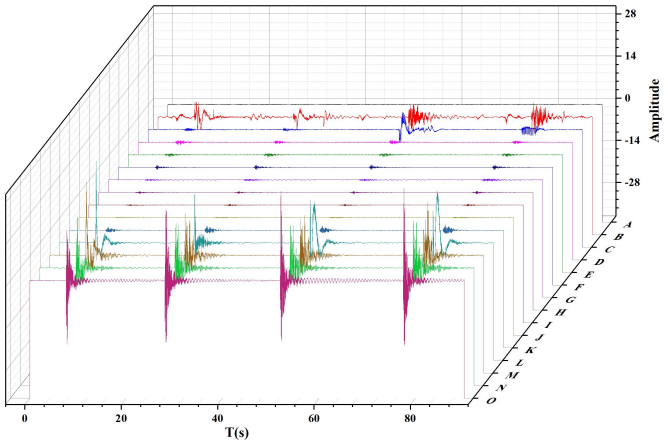

Fig. 8. Vibration Response When Striking Test Point O

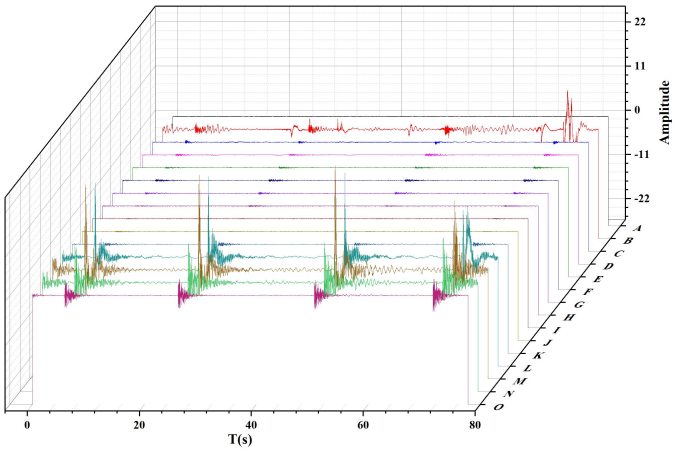

Fig. 9. Vibration Response When Striking Between Test Points M and L

Fig. 8 and 9 respectively illustrate the vibration responses observed when striking measurement point O and the region between measurement points M and L with a rubber mallet. In Fig. 8, it can be observed that all four main measurement points exhibit vibration responses when striking measurement point O. The amplitude of the response waveform at point O is higher than that of the other three points. Additionally, faint vibration responses can be observed at other locations along the track. Similarly, in Fig. 9, vibration responses are observed at all four main measurement points when striking between points M and L. The response waveforms at points M and L have similar amplitudes, which are higher than those at the other two points. Again, faint vibration responses can be observed at other measurement points along the track, although the amplitude of the response waveform at point O noticeably diminishes.

D. Test for different working conditions

During the test, the vibration of the track under different working conditions and static modes was tested, including: Fasteners fully tightened, unilateral failure of fasteners, bilateral failure of fasteners, failure of fastener intervals, all the fasteners failed, foreign invasion, pedestrian trespassing and environment noise.

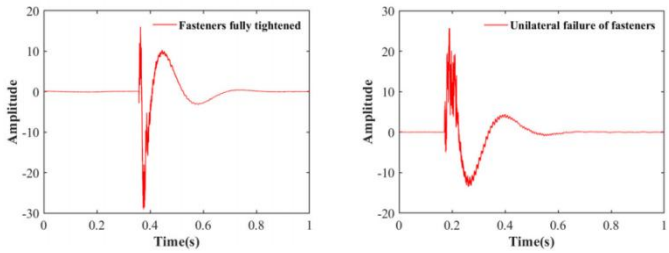

a) Fasteners fully tightened and unilateral failure of fasteners

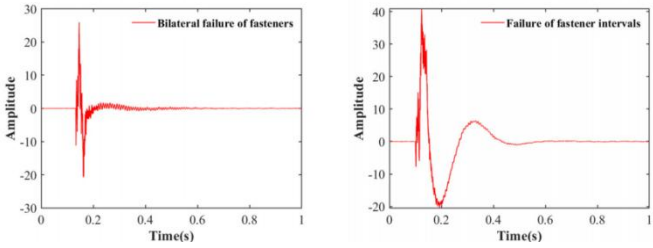

b) Bilateral failure of fasteners and failure of fastener intervals

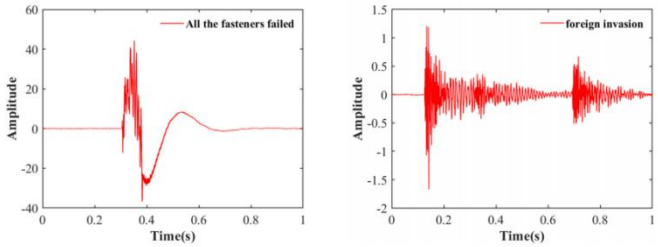

c) All the fasteners failed and foreign invasion

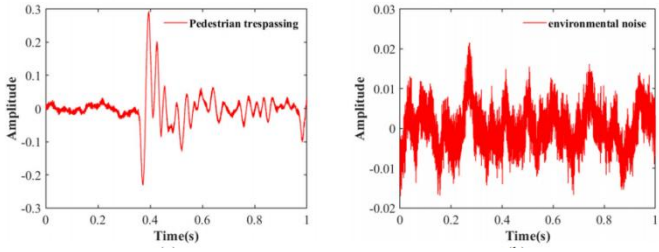

d) Pedestrian trespassing and environment noise

Fig. 10. The time domain of vibration signal under different conditions

As shown in Fig.10, a brief analysis of the rail vibration time-domain signals from the collected data shows that, the time-domain signal amplitude of foreign body intrusion and outside pedestrian intrusion is obviously smaller than that of fastener failure, and the difference is about an order of magnitude. Each working condition can not be distinguished directly by time-domain and frequency-domain signals, so it is necessary to analyze the vibration signals and extract the signal features for further verification and classification.

IV. Conclusion

In the current railway transportation systems, existing positioning methods often suffer from instability due to susceptibility to external environmental interference. To address this issue, this paper adopts weak fiber grating array

technology, which combines the insulation, strong anti-interference capability, and corrosion resistance of fiber Bragg gratings. A piezoelectric ceramic testing system is constructed and validated for its frequency response and phase amplitude. By establishing a field testing environment, the positioning effectiveness of the weak fiber grating array is evaluated. The results indicate that the weak fiber grating array installed on the railway can accurately perceive track vibrations, enabling vibration-based localization. In future research, this technology holds promise for applications such as train speed measurement, localization, foreign object intrusion detection, and track defect detection.

REFERENCES

[1] ZHANG M X. Research on the operation control system of medium and low speed maglev trains[D]. Chengdu:South West Jiaotong University, 2019: 24-56(in Chinese).

[2] GUI X, LI Zh Y, WANG H H, et al. Review of distributed sensing technology and application based on large scale grating array fiber [J]. Journal of Applied Science, 2021, 39(5): 747-776 (in Chinese).

[3] LIU H L, ZHU Zh W, ZHENG Y, et al. Experimental study on an FBG strain sensor [J]. Optical Fiber Technology, 2018, 40: 144- 151.

[4] ZHANG D P, LONG Zh Q, XUE S, et al. Optimal design of the absolute positioning sensor for a high speed maglev train and research on its fault diagnosis[J]. Sensors, 2012, 12(12): 10621-10638.

[5] LUO G B. Research on signal processing technology of high-speed maglev positioning and speed measurement system [D]. Changsha: National University of Defense Technology, 2017:47-106 (in Chinese).

[6] ZHU D F,WANG Y J,YANG Y, et al. Location and speed measurement method of urban rail train based on grating array [J]. Acta Photonica Sinica, 2019, 48(11): 1148014(in Chinese).

[7] WANG G, ZHANG M J, HUANG M G, et al. Research on load sensing system based on orthogonal fiber Bragg grating array[J]. Laser Technology, 2021, 45(2): 143-146 (in Chinese).

[8] LOUPOS K, AMDITIS A. Structural health monitoring fiber optic sensors[M]. New York,USA: Springer, 2017: 32-45.

[9] FILOGRANO M L, GUILLEN P C, RODRIGUEZBARRIOS A, et al. Real-time monitoring of railway traffic using fiber Bragg grating sensors[J]. IEEE Sensors Journal, 2012, 12(1): 85-92.

[10] WU Q F. Application research of train fiber Bragg grating monitoring system[D]. Beijing: Beijing Jiaotong University, 2015: 13-78 (in Chinese).

[11] QI X Sh, REN Zh G, LIU J Y, et al. Research on the influence of laser rust removal technology on the performance of collector rings of high-speed trains[J]. Laser Technology, 2019, 43 (2): 168-173 (in Chinese).

[12] YANG G, WANG Z Ch, YI L F, et al. A high-speed maglev train positioning system based on OFDR [J]. Communication and Information Technology, 2020(5): 72-85(in Chinese).

[13] DONG B, HE Sh Y,HU Sh Y, et al. Research on multiplexed sensing system based on tunable laser[J]. Laser Technology, 2005, 29(6): 608-610(in Chinese).

[14] LIU F, TONG X L, ZHANG C, et al. Multi-peak detection algorithm based on the Hilbert transform for optical FBG sensing [J]. Optical Fiber Technology, 2018, 45: 47-52.

[15] WANG M Y, SHENG L, KONG Y, et al. Research on the effect of laser linewidth on the performance of φ-OTDR system [J]. Laser Technology, 2016, 40(4): 615-618(in Chinese).